Available online at www.sciencedirect.com
SCIENCE DIRECT®
Physica A 357 (2005) 27–35
PHYSICA A
www.elsevier.com/locate/physa

Renormalized random walk study of oxygen absorption in the human lung

M. Filoche[a,b,*], M. Felici[a], B. Sapoval[a,b]

[a]*Laboratoire de Physique de la Matière Condensée, C.N.R.S. Ecole Polytechnique, 91128 Palaiseau, France*
[b]*Centre de Mathématiques et de leurs Applications, Ecole Normale Supérieure, 94140 Cachan, France*

Available online 20 June 2005

Abstract

Gas exchange at the acinar level involves several physico-chemical phenomena within a complex geometry. A gas transport model, which takes into account both the diffusion into the acinus and the diffusion across the alveolar membrane, is used to understand gas mixing in realistic systems. The behaviour of the system, first computed on model geometries in 3D finite elements method, can in fact be derived from the topological structure of the acinus only. A new efficient method based on random walks on a lattice is thus used to compute gas diffusion in structures taken from *real* morphological data. This approach shows that, at rest, the human acinus efficiency is only of 30–40%. These results provide a new evidence of the existence of diffusional screening at the acinar level, which means permanent spatial inhomogeneity of oxygen and carbon dioxide partial pressure. Application of these results to CO_2 clearance provides for the first time a theoretical support to the empirical relation between the O_2 and CO_2 partial pressures.

Keywords: Lung; Acinus; Diffusion; Screening; Simulation

*Corresponding author.
E-mail address: marcel.filoche@polytechnique.edu (M. Filoche).

0378-4371/$ - see front matter © 2005 Elsevier B.V. All rights reserved.
doi:10.1016/j.physa.2005.05.052

1. Introduction

The human lung is the organ in charge of the exchange of oxygen from air to blood and, conversely, of carbon dioxide from blood to air. This gas exchanges involve several physico-chemical process within a complex geometry. Convection insures the gas transport in the upper parts of the bronchial tree. In the distal regions of the lung called the *subacini* (eight subacini form an *acinus*, Fig. 1), oxygen is however moved at rest by molecular diffusion and then crosses the alveolar membrane to transfer into the blood [1]. From a physicist's point of view, the distribution of oxygen in the subacinus is the solution of a diffusion-reaction problem in an irregular space-filling structure in 3D [2]. For sake of simplicity, we will from now call acinus the elementary diffusion cell.

The mathematical model describing the acinus functioning at rest is the following. A fixed concentration C_0 is set at the acinus entry. As alveoli cover the acinar ducts walls, the absorbing interface is the entire system boundary. In the bulk, the current density $\vec{J}$ obeys Fick's law, $\vec{J} = -D\vec{\nabla}C$, where D is the diffusion coefficient of oxygen in air. At the interface, the current density is given by $J_n = -W(C - C_{blood})$, where the subscript n stands for the in-normal to the surface, C_{blood} is the

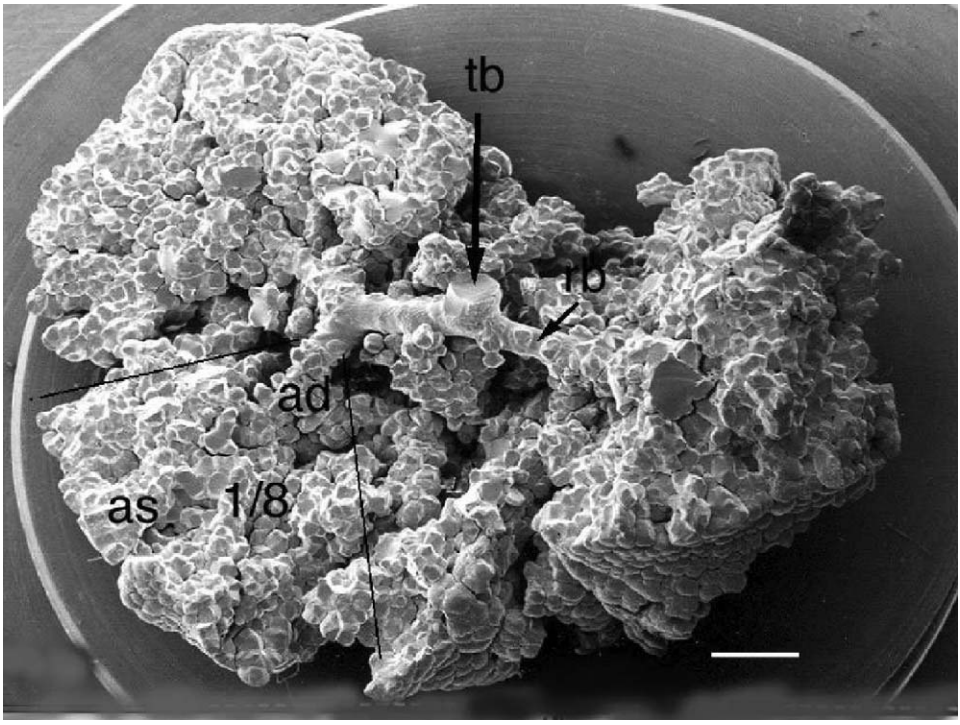

Fig. 1. Scanning electron micrograph of a silicon cast of a pulmonary acinus. The acinus is composed of eight subacini. White bar = 1 mm (courtesy of E. Weibel).

concentration of oxygen in the venous blood, and W the permeability of the membrane, defined as the flux per unit area and per unit concentration difference between the two sides of the membrane. In this first approach, the oxygen concentration in blood is set to a constant value [3,4]. In steady state, the conservation of the oxygen flux yields a Laplace equation for $\tilde{C} = C - C_{blood}$, $\nabla^2 \tilde{C} = 0$. Equating the bulk current density and the interface current density leads to a mixed boundary condition on the absorbing interface

$$\frac{\partial \tilde{C}}{\partial n} = \frac{\tilde{C}}{\Lambda} \quad \text{with} \quad \Lambda = \frac{D}{W} \,. \tag{1}$$

Note that the equations for the concentration are linear and hold both for oxygen uptake (with a source at the entry) and CO_2 clearance (where the source is located at the membrane surface).

In order to quantitatively measure the inhomogeneity of the distribution of the flux across the pulmonary membrane (a phenomenon also called *diffusional screening*), one can define the system efficiency η as the ratio of the real flux to the ideal flux obtained if no screening effects were present (infinite diffusivity or infinite Λ)

$$\eta(\Lambda_{O_2}) = \quad \frac{\Phi_{real}}{\Phi_{ideal}} = \frac{\int_{\text{acinar surface}} W_{O_2} \tilde{P}_{O_2} \, dS}{W_{O_2} \tilde{P}_{O_2}^{entry} S} \leqslant 1 \,. \tag{2}$$

This quantity is used to measure the fraction of the surface that is really active for gas exchange. It only depends on the unscreened perimeter length and on the geometry of the system. For this reason, we explicitly indicate the dependence on Λ_{O_2} by putting $\eta = \eta(\Lambda_{O_2})$.

2. Methods

We have applied the above mathematical description to simulate a 3D Kitaoka model acinus [5]. Kitaoka's algorithm generates intra-acinar pathways in a semi-stochastic way. The resulting 3D labyrinths show a mostly dichotomous branched structure with space-filling properties (Fig. 2). The acinar volume is schematized as a cube of side L, the alveolar ducts having a constant square section of side ℓ. To obtain the human $\frac{1}{8}$-subacinus, as described in Ref. [6], one must take $L = 3\,\text{mm}$ and $\ell = 0.5\,\text{mm}$, hence $L = 6\,\ell$.

Equations are solved through the finite elements method (FEM) on tetrahedral meshes. Unfortunately, the human subacinus is too large for such a computation: a sufficiently refined mesh (tetrahedron side of the order of $\ell/20$) would require millions of points. Still, a complete numerical solution can be computed for Kitaoka geometries of smaller size, $L = 3\,\ell$ and $L = 4\,\ell$.

The oxygen partial pressure in such a model acinus (size $L = 4\,\ell$, surface perimeter $L_P \simeq 64\,\ell$) is shown in Fig. 2 for an unscreened perimeter length $\Lambda_{O_2} = 256\,\ell$. As one can see, the distribution of oxygen partial pressure is far from uniform. In this case,

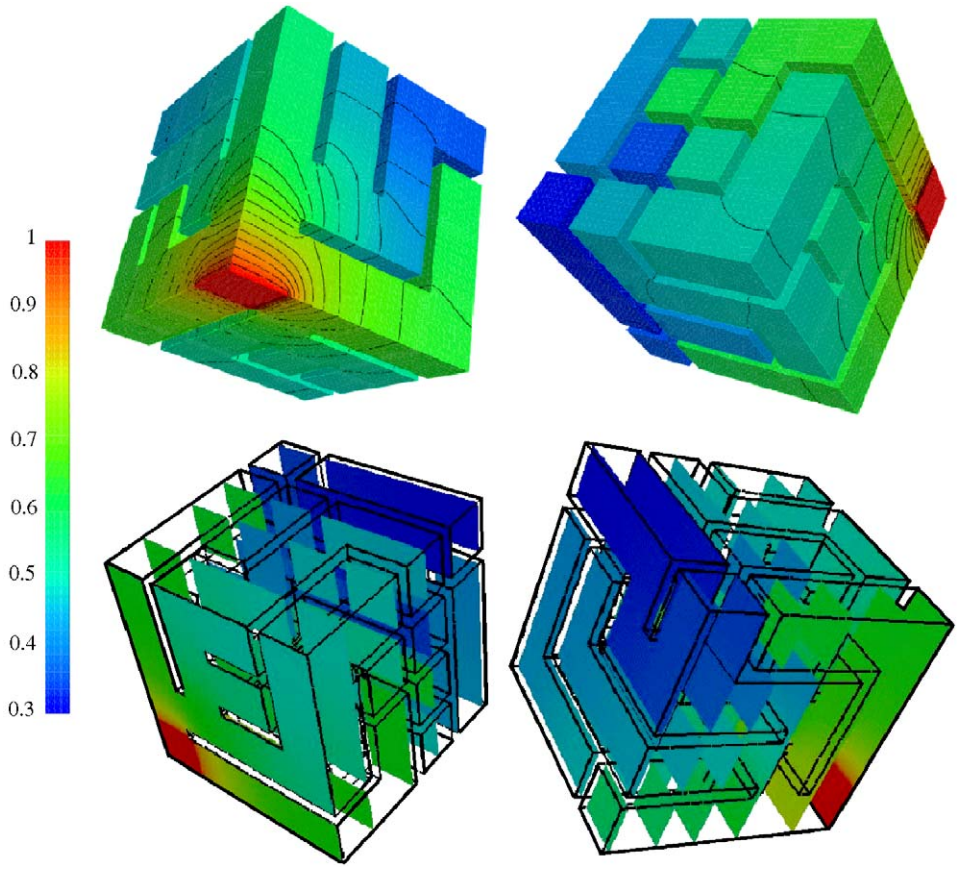

Fig. 2. Different views of oxygen partial pressure in the 3D Kitaoka model for $L = 4\ell$ for an unscreened perimeter length $\Lambda_{O_2} = 256\ell$. Top: oxygen partial pressure is plotted in colour. Black lines are isolevels of the partial pressure. Bottom: oxygen partial pressure in different planes within the 3D model.

the efficiency η is 51%. Now, in order to compute the diffusion of O_2 and CO_2 within a subacinus of realistic size, we have developed a new numerical method based on random walks. This method, called the *skeleton method*, has first been tested and calibrated with the 3D FEM simulations on smaller structures, and then used to compute the efficiency of realistic acini of size $L = 6\ell$.

2.1. The "skeleton method"

In the skeleton method, molecular diffusion is represented by random walks in a coarse-grained geometry. The skeleton of a 3D branched system can be defined as a tree with 1D branches, each branch representing an alveolar duct. Putting one site per unit distance ℓ, ℓ being the ducts diameter, one obtains a branching lattice. Fig. 3 illustrates this procedure in the case of a 2D branched system.

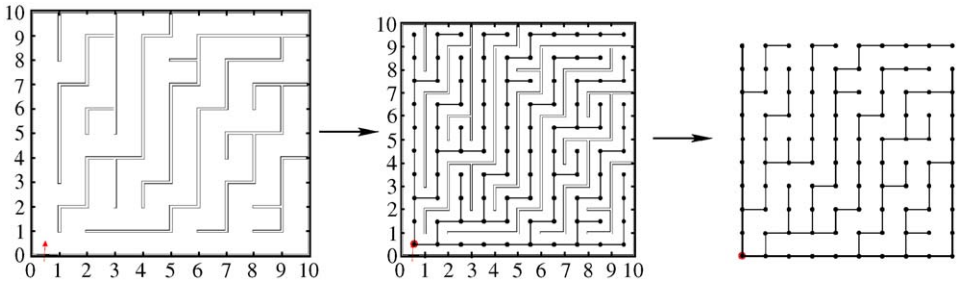

Fig. 3. Illustration of the skeleton method in 2D. Left: a bidimensional branched system (Kitaoka 2D model for $L = 10\ell$). Center: a skeleton is generated from the model. Sites are placed successively, at intervals equal to the duct diameter. For each site, one can define a coordination number n (number of lattice sites connected to the site itself). The number of absorbing walls surrounding a site is equal to $4 - n$ in 2D, and to $6 - n$ in 3D. Right: the resulting 2D skeleton.

Molecular diffusion of oxygen is simulated by a superposition of random walks on the lattice, starting from the entry. It is known that diffusion is the result of the many collisions of molecules causing random motion in space. Thus a great number of particles performing a random motion behave like a diffusing gas.

Absorption by the alveolar walls is included in the model. The walker moves along the tree or from site to walls, as follows: (i) one of the six directions of space (forward/backward, left/right, up/down) is chosen at random; (ii) if there is a neighbouring lattice site in this direction, the move is effective; (iii) otherwise, the walker collides with a wall site and is either absorbed with probability σ (and the walk ends) or reflected with probability $(1 - \sigma)$ to its original site and the walk goes on (Fig. 3).

The average occupation number of a lattice site i, k_i, is defined as the average number of times this site has been visited by a walker. To represent the oxygen mean concentration in a site, we consider $K_i = k_i/k_0$, k_0 being the average occupation number of the entry site. In this discrete representation, the efficiency η of the system can be defined as

$$\eta = \frac{\sum_i K_i s_i}{\sum_i s_i} \,. \tag{3}$$

Plots of the efficiency $\eta(\Lambda_{O_2})$ are presented in Fig. 4 (black symbols). In all cases, the efficiency varies as a power law for $\Lambda_{O_2} < L_P$ and slowly approaches 1 for $\Lambda_{O_2} \gg L_P$. On the left is presented a comparison between the FEM numerical simulations and the skeleton method for small acini. One can see that the skeleton method accurately reproduces the results of the direct 3D computation. On the right are shown eight different simulations of real topologies taken from Ref. [6], using the skeleton method. These simulations show that, at rest, the efficiency is comprised between 28% and 38%. It means that a large part of the exchange surface is not significantly used for oxygen transfer. Note also that, for a given value of Λ_{O_2}, the efficiency increases with decreasing acinus size: optimization of diffusional transport requires a

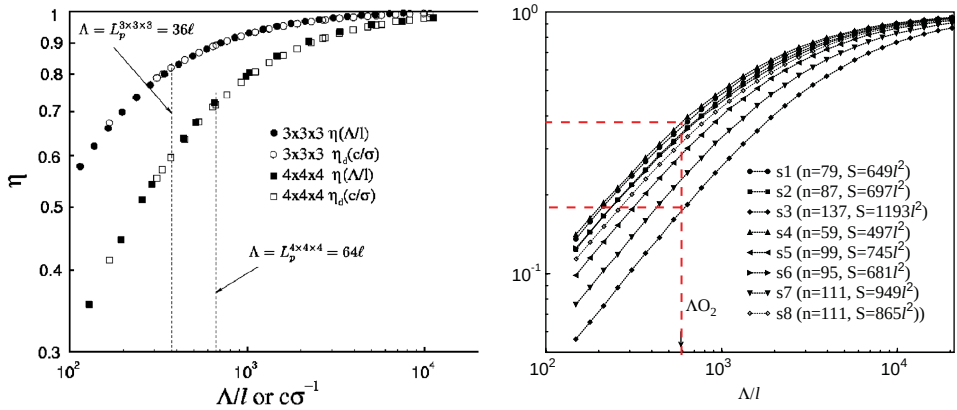

Fig. 4. (Left): comparison of the efficiency $\eta(\Lambda)$ obtained by the finite elements method (full symbols) and by the skeleton method (open symbols) for two sizes of the Kitaoka 3D acinus model (circles: $L = 3\,\ell$, $L_p \approx 36\,\ell$; squares: $L = 4\,\ell$, $L_p \approx 64\,\ell$). (Right): computation by the skeleton method of the efficiency for eight different subacini. The branching patterns are those of real subacini measured in Ref. [6]. The net result is that the efficiency at rest is roughly comprised between 30% and 40% (red lines).

small size. This result had already been asserted from numerical simulations in 2D [4] and is now confirmed for 3D systems [7].

3. Results and discussion

One can now interestingly compare the transfer of oxygen and carbon dioxide. The diffusivities D in air are approximately the same for O_2 and CO_2, whereas the membrane permeability is much larger for CO_2 (circa $\times 20$), due to the higher solubility of carbon dioxide in aqueous solutions. As a consequence, the unscreened perimeter length Λ is smaller for CO_2 and the acinus is *much less* efficient for CO_2 clearance than for O_2 uptake. The net result is that the flux *per unit partial pressure difference* for CO_2 (proportional to $\eta(\Lambda) \times W$) is not 20 times but only 2.5 times larger than the corresponding value for O_2 (see Eq. (4)).

The two cases are illustrated in Fig. 5. The O_2 and CO_2 partial pressure distributions in a 2D Kitaoka model acinus are compared for $\Lambda_{O_2} = 800\,\ell$ and $\Lambda_{CO_2} = \frac{1}{20}\Lambda_{O_2}$. As one can see, the CO_2 partial pressure is uniform and maximal (i.e., at equilibrium with blood) in most of the volume, while $\tilde{P}_{CO_2}$ is appreciably different from zero only near the entry.

In respiratory physiology, a commonly used concept is that of an "alveolar gas" characterized by uniform partial pressures of the different gases. Although the above considerations show that the distribution of oxygen and carbon dioxide are not homogeneous in the acinus, we now show that this diffusion model allows to predict the value partial pressure of oxygen in the venous blood. One must first choose the values of the partial pressures at the input and output of the lung compartment. One

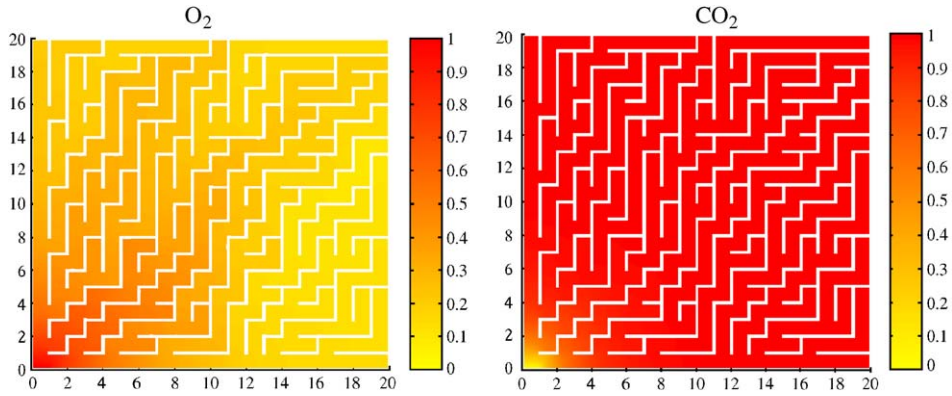

Fig. 5. Oxygen and carbon dioxide distribution in a 2D Kitaoka acinus. Left: oxygen partial pressure $P_{O_2}(\vec{x})$ for $\Lambda_{O_2} = 800\,\ell$; Right: carbon dioxide partial pressure $P_{CO_2}(\vec{x})$ for $\Lambda_{CO_2} = 40\,\ell$. In most of the acinus, the CO_2 partial pressure is very close to the blood CO_2 partial pressure and the flux is very small. The active region (where the gradient is different from zero) is located near the entrance (lower left corner), as for oxygen, but it is much smaller.

may assume for the partial pressures at input those in the mouth: $P_{O_2}^{entry} = 150\,\text{mmHg}$ and $P_{CO_2}^{entry} = 0.3\,\text{mmHg}$. This gas is saturated with water vapour.

At the output, one must choose the blood partial pressure of CO_2, which we suppose uniform. In the mixed venous blood, which is pumped by the heart to the alveoli, the CO_2 partial pressure varies between 43 and 47 mmHg: we choose the mean value $P_{CO_2}^{blood} = 45\,\text{mmHg}$. Lastly, we assume that the O_2 and CO_2 fluxes are equal, as they must be in the steady state. This gives

$$\frac{\tilde{P}_{O_2}^{entry}}{\tilde{P}_{CO_2}^{entry}} = \frac{W_{CO_2}\eta(\Lambda_{CO_2})}{W_{O_2}\eta(\Lambda_{O_2})} = 2.5\,. \tag{4}$$

Given $P_{O_2}^{entry}$, $P_{CO_2}^{entry}$ and $P_{CO_2}^{blood}$, Eq. (4) yields for $P_{O_2}^{blood}$ the value $P_{O_2}^{blood} = 38.5\,\text{mmHg}$. Remarkably, this value, obtained from a screening theory, is very close to the measured value in the mixed venous blood which is around 40 mmHg.

The general agreement between the partial pressures in the two models leads us to propose a new physiological model for the acinus, in which $P_{O_2}(\vec{x})$ decreases smoothly from $P_{O_2}^{entry} = 150\,\text{mmHg}$ at the subacinus entry to a minimum of 40 mmHg in the less accessible regions of the system (Fig. 6).

Let us now consider the breathing of a mixture which is not air but Heliox: in this case, oxygen is mixed with helium instead of nitrogen. Collisions against the lighter molecules are less efficient for scattering, so that the oxygen diffusion coefficient is larger in this mixture than in air. This increases the unscreened perimeter length, whereas the permeability remains constant. Efficiency increases by a factor of 2. Similarly, the replacement of N_2 by He favours carbon dioxide clearance.

In the case of pure oxygen breathing, diffusion screening is absent. $\tilde{P}_{O_2}$ is maximal everywhere, and oxygen uptake is increased. However, diffusion screening is present

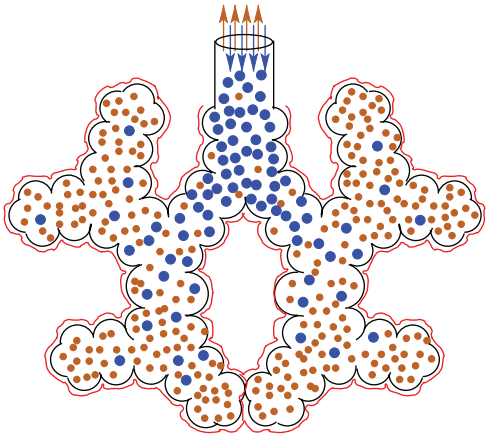

Fig. 6. Scheme of the subacinus at work. Oxygen is depicted in blue and carbon dioxide in brown. The oxygen partial pressure is maximal at the entry of the subacinus. It decreases smoothly towards the distal regions of the acinar volume because of diffusional screening. In contrast, carbon dioxide is rather homogeneously distributed in the acinar volume except for a small region near the entry.

for CO_2, as the diffusion coefficient D_{CO_2,O_2} differs little from $D_{CO_2,air}$ and all other quantities are the same as in air.

4. Conclusion

A physical model of the gas diffusion in the acinus has been proposed. This model allows to quantitatively evaluate the inhomogeneity of oxygen and carbon dioxide partial pressures within the acinus. First, the effects of diffusional screening in the human pulmonary acinus have been studied numerically using direct 3D numerical simulations. We have shown that the acinus efficiency is determined by its branching pattern only. It is therefore possible to perform simulations on simplified tree-like lattices designed on the acinus branching pattern. Random walk simulations on such lattices give the same quantitative result than direct numerical computation of the solution of the diffusion equations in the corresponding 3D geometries. This approach allows one to compute the efficiency of real human acini much more easily.

The net result is that, at rest, the efficiency of the human acinus is of order 30–40%. This is because the partial pressure distribution in the subacinus is not homogeneous. It decreases from the entry to the deeper regions, whereas carbon dioxide partial pressure is rather high and homogeneous everywhere except at the entry. One should stress that the existence of this inhomogeneity is *not* the consequence of an insufficient diffusion velocity during inspiration. Remarkably, the same theoretical frame applies quantitatively to both oxygen uptake and carbon dioxide clearance. It permits to predict, without any adjustable parameter, the value of the partial pressure of oxygen in venous blood from the partial pressure of CO_2.

At last, this model gives some insights about the breathing of other gas mixtures such as Heliox or pure oxygen, which can be explained by the existence of diffusional screening. In order to obtain more precise estimations, one should reconsider the approximations that have been made, especially the assumption of constant blood pressures. Note also that the convection-diffusion transition has been dealt in a very approximate way, as being abrupt and located at the subacinus entry.

Acknowledgements

We wish to thank E. Weibel, T. Similowski and C. Straus for our numerous discussions about this work.

References

[1] E.R. Weibel, The Pathway for Oxygen, Harvard University Press, Cambridge, MA, 1984.
[2] B. Sapoval, Transfer to and across irregular membranes modelled by fractal geometry, in: T.F. Nonnenmacher, G.A. Losa, E.R. Weibel (Eds.), Fractals in Biology and Medicine, Birkhäuser-Verlag, Bâle, 1994.
[3] B. Sapoval, M. Filoche, E.R. Weibel, Smaller is better-but not too small: a physical scale for the design of the mammalian pulmonary acinus, Proc. Natl. Acad. Sci. 99 (2002) 10411–10416.
[4] M. Felici, M. Filoche, B. Sapoval, Diffusional screening in the human pulmonary acinus, J. Appl. Physiol. 94 (2003) 2010.
[5] H. Kitaoka, S. Tamura, R. Takaki, A three dimensional model of the human pulmonary acinus. J. Appl. Physiol. 88 (2000) 2260–2268.
[6] B. Haefeli-Bleuer, E. Weibel, Morphometry of the human pulmonary acinus, Anat. Rec. 220 (1988) 401–414.
[7] M. Felici, Physique du transport diffusif de l'oxygène dans le poumon humain, Ph.D. Thesis, Ecole Polytechnique, Palaiseau, France, 2003.